Feature Article:

DOI. No. 10.1109/MAES.2022.3141436

Hybrid Perturbations in Stacked Patch–Ring Circularly Polarized Microstrip Antennas for CubeSat Applications

M. Mubasshir Hossain, Saeed I. Latif, and Edmund A. Spencer, **University of South Alabama, Mobile, AL 36688, USA**

INTRODUCTION

Modern satellite communication demands a high data transmission rate and increased payload. In order to achieve greater data transfer to ground stations and other satellites, onboard antennas with large bandwidths are required. The link budget dictates the choice between higher output power from the transceiver or higher antenna gains. Due to the limiting factor of dc power on small satellites, high antenna gains are preferred. Also, the constraints from small space and mass budgets in CubeSats pose challenges for installing high-profile onboard antennas for successful wireless communication. For this reason, the communication engineers or researchers of any small satellite mission always look for an optimum combination of available ground stations and onboard antennas with the best possible parameters. While earlier CubeSat missions mostly relied on UHF communication bands using deployable wire antennas [1], current science missions utilizing CubeSats to perform sophisticated science experiments demand the use of high frequencies, such as *S*- or *X*-bands to tackle increased data volume. NASA's Deep Space Network (DSN) and Near Earth Network (NEN) are the two of the world's strongest ground station networks in their respective operating regions. DSN's *S*-band receiving frequency range is 2200–2300 MHz [2] and NEN's 13 different ground stations antennas also receive 2200–2300/2400 MHz [3], which can be considered with confidence for CubeSat telemetry, tracking, and control, and science data download for any CubeSat projects.

An important requirement in satellite communication is the large beamwidth circularly polarized (CP) radiation. CP antennas do not require strict orientation between transmitter and receiver and are very effective in combating fading caused by the Faraday rotation effect in the ionosphere [4]. They are very popular in the applications, such as Global Positioning System, Global Navigation Satellite System, Radio Frequency Identification, and Wireless Local Area Network [4], and are being widely used in CubeSat applications. In high-frequency CubeSat applications, patch antennas can be used because of their ease of fabrication, smaller size, conformity to curved surfaces, and low cost [5].

An innovative antenna design accommodates wide beamwidth, wideband circular polarization radiation, high gain, and selected frequency bandwidth at a low elevation that a satellite communication usually demands. CP antennas are special types of antennas that require a mechanism to generate nearly equal orthogonal currents with 90° phase difference. CP in microstrip antennas can be achieved either by using dual orthogonal feeds or by introducing perturbations when a single feed is used. Conventional single-layer, singly fed microstrip CP antennas inherently have narrow bandwidth and poor angular coverage. A stacked patch antenna configuration offers wider impedance bandwidth compared to other design techniques. Stacked ring patches with hybrid perturbations have demonstrated the ability to widen impedance and axial ratio (AR) bandwidths using a single probe feed [6]. The perturbation is introduced in the form of cutting diagonal corners called negative perturbation or adding metal stubs to the diagonal corners, known as positive perturbations.

In this work, the hybrid perturbation approach is employed to accomplish CP from dual layer stacked ring–patch antennas. First, stacked driven patch and parasitic ring, both with negative perturbations, are used to achieve wide impedance and AR bandwidths. Then, the driven

Authors' current address: M. Mubasshir Hossain, Saeed I. Latif, and Edmund A. Spencer are with the University of South Alabama, Mobile, AL 36688, USA (e-mail: mh1934@jagmail.southalabama.edu; slatif@southalabama.edu; espencer@southalabama.edu).

Manuscript received January 23, 2021; accepted December 1, 2021, and ready for publication January 6, 2022.

Review handled by Richard Linares.

0885-8985/22/$26.00 © 2022 IEEE

Image licensed by Ingram Publishing

patch is positively perturbed and the parasitic ring is negatively perturbed so that the overall size of the antenna is not increased, but wider angular beamwidth can be obtained. The proposed design technique is analogous to the concept of sequential rotation in arrays, where elements are physically rotated to improve the AR beamwidth. Both left-hand circular polarization (LHCP) and right-hand circular polarization (RHCP) can be achieved by appropriately choosing the positions of perturbations in a patch [6]. In this article, only the RHCP is targeted. The ''Design and Implementation of the Antennas'' section describes the design of two antennas: the stacked ring–patch antenna with negative perturbations on both the driven and the parasitic elements, and the stacked ring–patch antenna with hybrid perturbations on the driven and the parasitic elements. The performances of both antennas are compared in the ''Performance Comparison'' section. The antenna performances are investigated by placing the antenna on a CubeSat and a parametric study is presented in the ''Antenna Performance on a CubeSat and Parametric Study'' section. Experimental results are discussed in the ''Experimental Study'' section. Finally, the "Conclusion" section concludes this article.

DESIGN AND IMPLEMENTATION OF THE ANTENNAS

RING–PATCH STACKED CONFIGURATION WITH NEGATIVE PERTURBATIONS

A singly fed ring–patch antenna is a miniaturized version of the patch antenna, since it provides a longer current flow path compared to that in a solid patch. A CP patch antenna in the *S*-band is designed for CubeSat applications that exploit a patch–ring combination in a stacked setup. The first step is to design an antenna to operate in the *S*-band so that NASA's ground station networks can be utilized for downlink communication. In the second step, circular polarization is achieved by introducing perturbation segments to the patch and the ring elements. The shape and the dimensions of the perturbations are optimized to ensure that the antenna achieves an AR that is below 3 dB in the desired design frequency band. Within this band, it is also targeted to achieve wide AR beamwidth for wide angular coverage. Figure 1 shows the antenna geometry and design, with the basic antenna design parameters tabulated in Table 1. It comprises three metal layers and two dielectric layers. The driven patch, one of three metal layers, is on a grounded dielectric substrate: Rogers TMM3 with permittivity $\varepsilon_r = 3.27$ and thickness $h_1 = 1.524$ mm. The TMM3 substrate is the first dielectric layer. The driven patch is excited by a 50-Ω SMA probe at a point (X_F, Y_F).

The parasitic ring is electromagnetically coupled to the driven patch, and is separated from it by a foam substrate, the second dielectric layer. It has a permittivity close to the air. The height of the foam substrate h_2 is critical for ensuring effective coupling between two resonators. The width

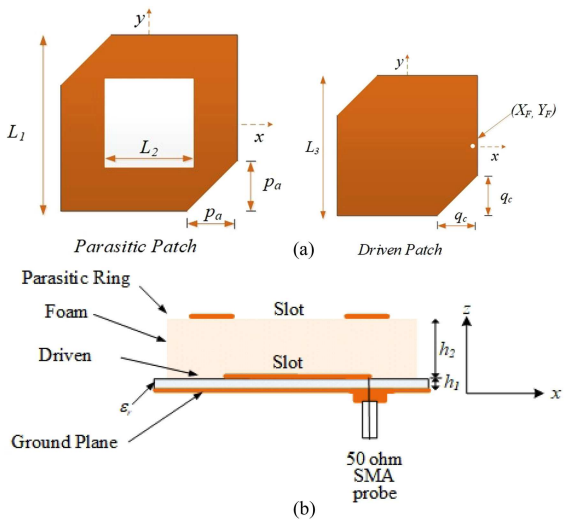

Figure 1.
Geometry of the ring–patch antenna with negative perturbations. (a) Top view. (b) Side view.

Table 1.

Design Parameters of the Stacked Square Ring–Patch Antenna With Negative Perturbations for CP				
Parasitic ring size (mm)	**Driven patch size (mm)**	**Corner perturbation (mm)**	**Probe position (mm)**	**h_2 (mm)**
$L_1 = 41$	$L_3 = 36.8$	$p_a = 5.9$	$X_F = 17.6$	11
$L_2 = 27.8$		$q_c = 7.4$	$Y_F = 0$	

of the ring is W, which represents the amount of miniaturization and determines the actual size of the antenna along with the ground plane. The dimensions of the square patch and the square ring are carefully chosen so that the resonances are close enough to provide a wideband operation. The driven patch and the parasitic ring have been carefully perturbed to generate CP. Corner cuts on both the ring and the patch, denoted by p_a and q_c, as shown in Figure 1, create two degenerated modes, which are orthogonally polarized to each other. In order to generate the RHCP, the perturbations have to be on the diagonal corners along $\phi = 135^o$ line. If an LHCP is desired, corner cuts have to be placed on the corners along $\phi = 45^o$ line.

A finite ground plane is used in the simulation, and modeling of the designed ring–patch antenna, the size of which is 60×60 mm^2. It can be shown from the dimensions of the antenna that the average circumferential length of the ring is about one wavelength on the foam substrate and the patch size is half-wavelength in the dielectric substrate. The driven patch is excited by a 50-Ω SMA probe at the point ($X_F = 17.6$, $Y_F = 0$), as shown in Figure 1. Figure 2 shows the simulated S_{11} plot of the ring–patch stacked antenna with negative perturbations. A wideband $S_{11} <$ -10-dB bandwidth from 2140 to 2470 MHz (14.3%) has been achieved, which covers the required CP bandwidth to be used with the NEN and DSN. Figure 3 represents the AR and RHCP gain versus frequency plots of the antenna. The antenna has a good

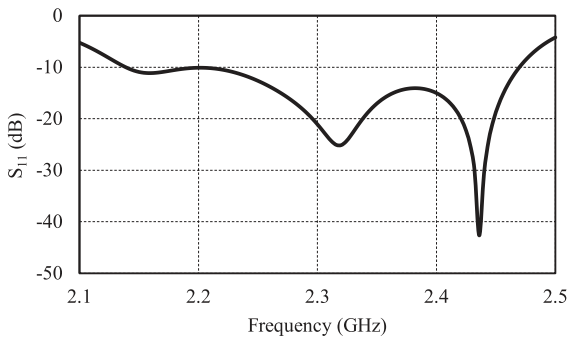

Figure 2.
Simulated S_{11} plot of the proposed antenna with negative perturbations.

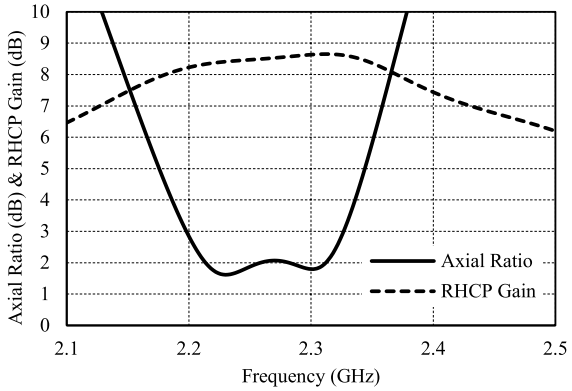

Figure 3.
AR and RHCP gain versus frequency plot of the proposed antenna with negative perturbations.

3-dB AR bandwidth of 5.65% (2198–2326 MHz) compared to a mere 1% bandwidth from a single-layer single probe-fed CP microstrip patch antenna [7], [8]. Two minima in the AR plots depict the wideband CP nature of this antenna. The first minimum has an AR value of 1.6 dB at 2232 MHz, which is due to the parasitic ring, and the second one has 1.79 dB at 2300 MHz due to the driven patch. The antenna has a high RHCP gain of 8.2–8.6 dB within the CP bandwidth, which is higher than that from a typical single-layer CP microstrip patch antenna. The RHCP gain along boresight is 8.41 and 8.63 dBic at 2232 and 2300 MHz, respectively, in both principal planes.

RING–PATCH STACKED CONFIGURATION WITH HYBRID PERTURBATIONS

In order to improve the beamwidth, hybrid perturbations instead of negative perturbations are applied to this patch–ring stacked antenna. The geometry of the configuration is shown in Figure 4. For the hybrid perturbation scheme, all the dimensions of W_1, W_2, W_3, q_a, and p_c are kept fixed for the best possible AR bandwidth, impedance bandwidth, and radiation pattern characteristics. The driven patch is fed with a 50-Ω SMA probe at the point $X_F = 16.1$ and $Y_F = 0$ mm. The height h_2 or the layer separation is kept at 11 mm, similar to the previous case. The dimensions of the square patch and the square ring are carefully chosen so that the resonances are close enough to provide wide impedance and AR bandwidths. The driven square patch and the parasitic square ring are carefully perturbed to generate RHCP. Negative perturbations are introduced to the diagonal corners of the ring in the form of cuts. These are denoted by p_c in Figure 4.

Added stubs at the other diagonal corners on the driven patch are positive perturbations and are denoted by q_a. These perturbations create two degenerated modes, which are orthogonally polarized with each other and create RHCP. In order to generate the LHCP, the perturbations have to be on

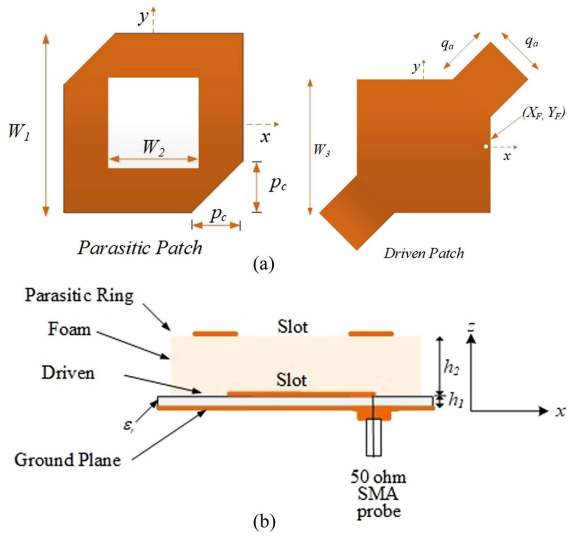

Figure 4.
Geometry of the proposed ring–patch stacked antenna with hybrid perturbations. (a) Top view. (b) Side view.

the diagonal corners along $\phi = 135^{o}$ line on the driven patch and along $\phi = 45^{o}$ line on the parasitic ring.

If an LHCP is desired, corner cuts have to be placed at the corners along the $\phi = 45^{o}$ line on the parasitic ring. A finite ground plane is used in the simulation a, the size of which is 60 × 60 mm^2. The optimized design parameters of the proposed antennas, for wideband operation, are shown in Table 2. The simulated S_{11} plot of the antenna is shown in Figure 5. It is observed that for the hybrid method, the simulated impedance bandwidth for $S_{11} < -10$ dB is 312 MHz (13.6%) ranging from 2140 to 2452 MHz. However, it shows a wider 3-dB AR bandwidth of 6.81% ranging from 2184 to 2338 MHz. The first minimum AR value is 1.17 dB at 2.216 GHz, which is due to the parasitic ring. The second one is 1.18 dB at 2.312 GHz, which is due to the driven patch. The RHCP gain over the CP bandwidth is 8.3–8.8 dB. The simulated RHCP gain along boresight is 8.47 and 8.76 dBic at 2216 and 2312 MHz, respectively, in both principal planes. Figure 6 shows the simulated AR and RHCP gain versus frequency plots of the stacked antenna with hybrid perturbations.

Table 2.

Design Parameters of the Stacked Square ring–Patch Antenna With Hybrid Perturbation				
Parasitic ring size (mm)	Driven patch size (mm)	Corner perturbations (mm)	Probe position (mm)	h_2 (mm)
$W_1 = 42.2$	$W_3 = 34$	$p_c = 3$	$X_F =$ 16.1	11
$W_2 = 26.3$		$q_a = 5$	$Y_F = 0$	

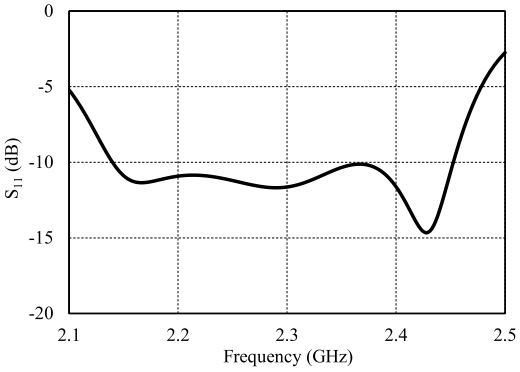

Figure 5.
Simulated S_{11} plot of the proposed antenna with hybrid perturbations.

PERFORMANCE COMPARISON

For both antennas, the S_{11} plots show multiple resonances from two resonators, which are judicially combined to achieve wide impedance bandwidth. The impedance bandwidth obtained is greater than that for the CP antenna with ring–ring combination presented in [6], and the CP antenna presented in [9] and [10]. A comparison of this bandwidth and other data is summarized in Table 3.

It has been found that the percentage AR bandwidth from the stacked ring–patch antenna with hybrid perturbations is wider than that with negative perturbations. An enhanced AR beamwidth is achieved with the hybrid design, which can be visualized by looking at the variations of AR with the elevation angle for both cases presented in Figure 7. Here, they are plotted at their respective first and second AR minima points in the $\varphi = 0°$ plane. The first AR minima points are 2216 MHz for the hybrid case and 2232 MHz for the negative case. Figure 7(a) shows the AR versus elevation angle plots for the first AR minima points. It can be noticed that the hybrid antenna has a wider angular coverage, for which the 3-dB AR beamwidth is 106°, from -53° to +53° off

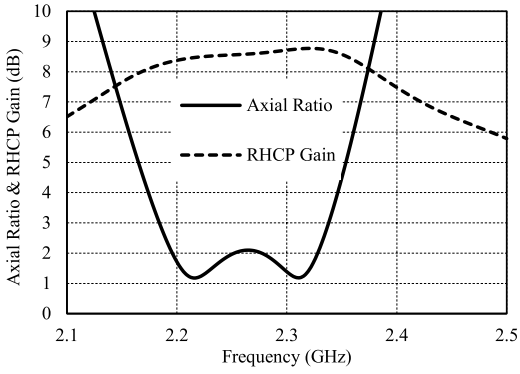

Figure 6.
AR and RHCP gain versus frequency plot of the proposed antenna with hybrid perturbations.

Table 3.

Performance Comparison of the Proposed Antenna With Stacked CP Antennas Having Ring–Patch Configuration, and Other Single-Layer CP Microstrip Antennas

Antennas	Operating frequency (GHz)	ε_r	Impedance bandwidth	AR bandwidth	Peak gain (dBic)
Proposed negative	2.25	3.2	14.32% (2140–2470 MHz)	5.65% (2198–2326 MHz)	8.63
Proposed hybrid	2.25	3.2	13.6% (2140–2452 MHz)	6.81% (2184–2338 MHz)	8.76
Ref. [6]	1.6	3.2	10.8% (1510–1683 MHz)	5% (1545–1624 MHz)	9
Ref. [9]	2.3	3.55	11.5% (2220–2490 MHz)	6% (2260–2400 MHz)	11
Ref. [10]	2.4	4.4	12.08% (2266–2562 MHz)	6.6% (2380–2543 MHz)	4.5

the boresight. The angular coverage for the stacked ring–patch antenna with negative perturbations is only 62°, from -31° to +31°, off the boresight.

Figure 7(b) shows the same plots for both antennas at their second AR minima points. Table 4 presents the AR beamwidths for both cases.

Circular polarization gain plays one of the prime roles in selecting an antenna for satellite communications. Ring–patch antennas with negative and hybrid perturbations provide 2–3 dB higher CP gains than those from typical patch antennas because of the stacked configuration.

Figure 8 represents the comparison between RHCP gains of these antennas at their respective first and second AR minima points in the $\varphi = 0°$ plane. The RHCP

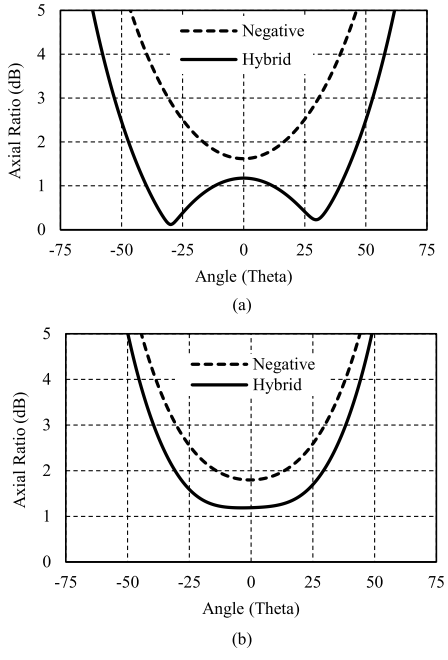

Figure 7.
Variation of the AR with the elevation angle in the $\phi = 0°$ plane of the proposed antennas. (a) At first minima AR points (hybrid perturbations: 2216 MHz and negative perturbations: 2232 MHz). (b) At second minima CP points (hybrid perturbations: 2312 MHz and negative perturbations: 2300 MHz).

gains of the stacked ring–patch antenna with hybrid perturbations at its first AR minimum frequency (2216 MHz) are 8.47 dBi and at its second AR minimum frequency (2312 MHz) is 8.76 dBi. Similarly, the RHCP gain of the stacked ring–patch antenna with negative perturbations at its first AR minimum frequency (2232 MHz) is 8.41 dBi, whereas at its second AR minimum frequency (2300 MHz) is 8.63 dBi.

Cross-polarization also carries a major importance in satellite communications. Each mission has its own defined maximum cross-polarization value. It is observed that hybrid perturbations on the stacked ring–patch antenna provide a lower cross-polarization than that in the stacked ring–patch antenna with negative perturbations. In the hybrid case, the cross-polarization (LHCP gain) level is below -15 dB from -51° to +51° elevation angle at its first minima, whereas this value is between -8 and -12 dB in the negative perturbations case for the same range of angle, as can be noticed in Figure 9(a). Similar performance can be noticed in Figure 9(b) for the second minima.

ANTENNA PERFORMANCE ON A CUBESAT AND PARAMETRIC STUDY

To check the compatibility of the designed antenna with a CubeSat, the antenna parameters are checked under several possible conditions through simulations. First, 1U,

Table 4.

3-dB AR Beamwidth Comparison Between Ring–Patch Antenna With Hybrid Perturbation and Ring–Patch Antenna With Negative Perturbation

Antennas	At first AR minima	At second AR minima
	$\varphi = 0°$	$\varphi = 90°$
Hybrid	106° (-53° to +53°)	78° (-40° to +38°)
Negative	62° (-31° to +31°)	60° (-30° to +30°)

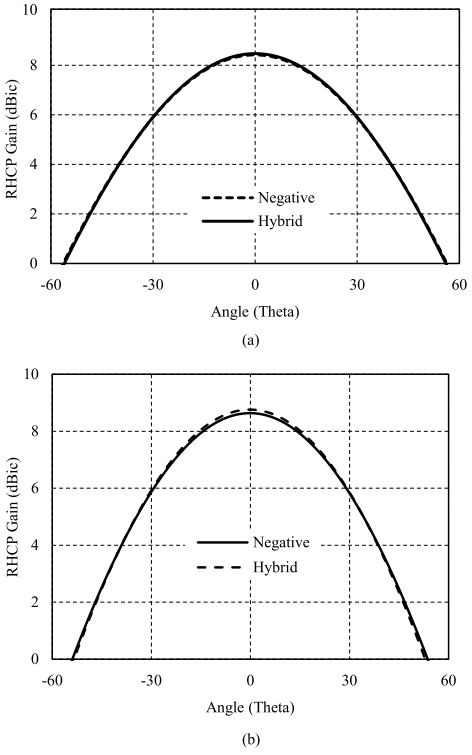

Figure 8.
RHCP gain patterns in the $\phi = 0^\circ$ plane. (a) At first AR minima points of the antennas. (b) At second AR minima points of the antennas.

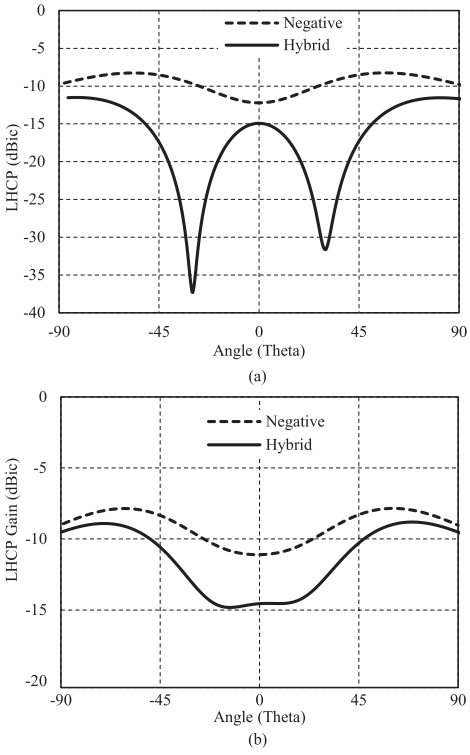

Figure 9.
LHCP gain patterns in the $\phi = 0^\circ$ plane. (a) At first AR minima points of the antennas. (b) At second AR minima points of the antennas.

2U, and 3U CubeSat structures are considered with one CP stacked antenna on top, as shown in Figure 10. A glass insulation with 2-mm thickness between the antenna and the CubeSat is used. A perfect electric conductor connection between the antenna ground and the CubeSat is maintained to keep the CubeSat RF circuit ground and the antenna ground the same. The impedance bandwidth is almost the same for all three cases (1U, 2U, and 3U). Also, in 1U and 3U cases, the AR bandwidths are almost the same as those of the designed antenna on a regular ground plane, from 2185 to 2328 MHz, as shown in Figure 11(a). However, in the 2U case, there is a shift in the frequency of operation by 8 MHz, although the overall AR bandwidth is almost the same. Therefore, it can be concluded that the antenna behaves very similarly when used with CubeSats. The stacked ring–patch antenna is also simulated without the glass insulator. In this case, the top surface of the CubeSat acts as the antenna ground plane. Several antenna dimensions, including the substrate and the foam layer sizes, and positive and negative perturbations are varied. A 2U CubeSat was considered for this study. When the dimensions of the dielectrics are varied, the impedance bandwidth remains the same. No drastic change in the AR bandwidth was observed for this variation, as shown in Figure 11(b).

Figure 12(a) shows the AR comparison for varying the positive perturbations (q_a) on the driven patch (bottom patch). It can be noticed that this parameter affects more on the second CP resonance than the first one. As q_a becomes larger, the operating frequency shifts to the lower frequency. The positive perturbation affects the impedance bandwidth as well. Therefore, an optimization process is required to obtain the best impedance and AR bandwidths. Figure 12(b) shows the AR comparison for varying the negative perturbation (p_c) on the parasitic patch (upper patch). This parameter affects both AR and impedance bandwidths less significantly compared to the positive perturbations on the driven patch case. Negative perturbations make the ring smaller, and as such the CP resonances shift to higher frequencies. Again, an optimized q_c is required for obtaining the largest AR bandwidth with good impedance matching.

EXPERIMENTAL STUDY

A prototype of the stacked ring–patch antenna with hybrid perturbations was fabricated in the Applied Electromagnetics Research Lab, University of South Alabama, using heat press printing and chemical copper etching processes.

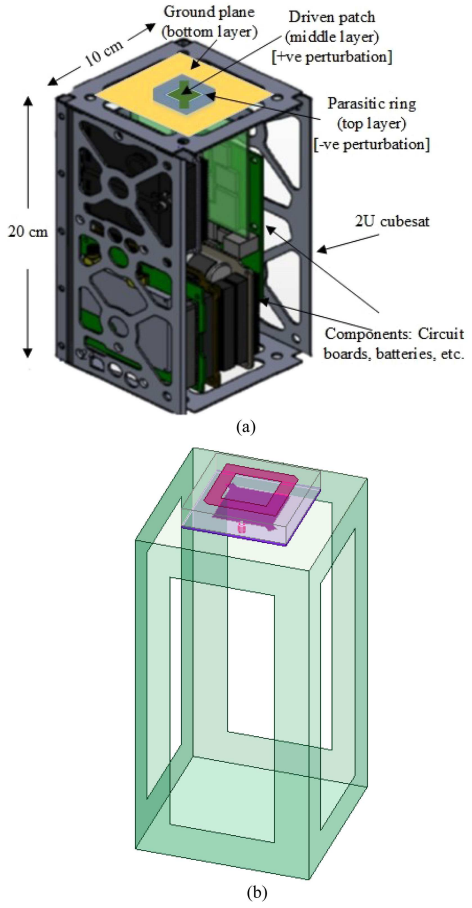

Figure 10.
(a) Proposed hybrid antenna on a 2U CubeSat. (b) Simulation model for the antenna with a 2U CubeSat.

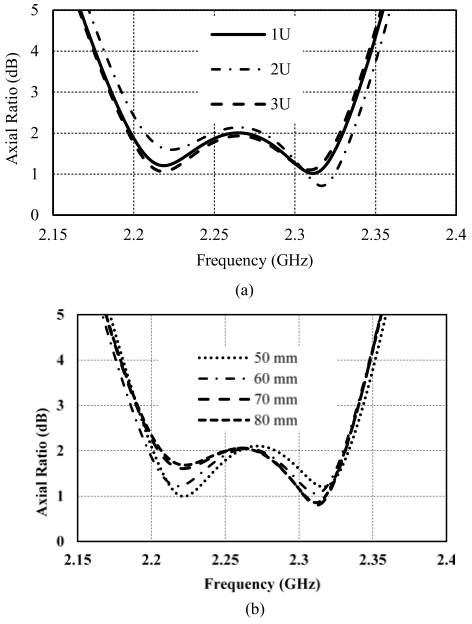

Figure 11.
AR comparison. (a) Changing the size of the CubeSat. (b) Changing the substrate dimension on a 2U CubeSat.

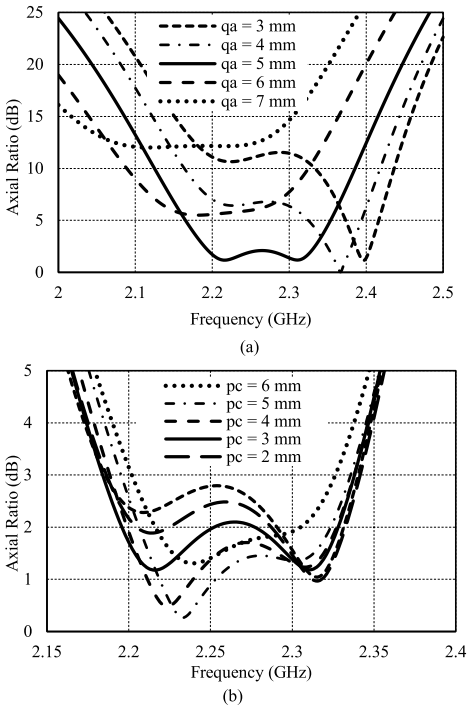

Figure 12.
(a) AR versus frequency plots varying the positive perturbation. (b) AR versus frequency plots varying the negative perturbation.

Photographs of the driven patch and the parasitic ring are shown in Figure 13. The antenna scattering parameters were measured in a Wiltron 37369A 40 MHz–40 GHz Vector Network Analyzer. The measured S_{11} < -10 dB

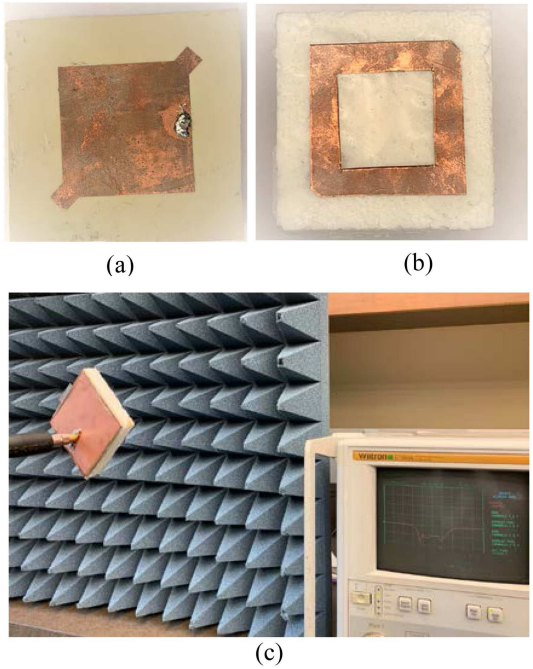

Figure 13.
(a) Driven patch of the fabricated antenna. (c) Top view of the fabricated antenna. (c) Fabricated antenna under test.

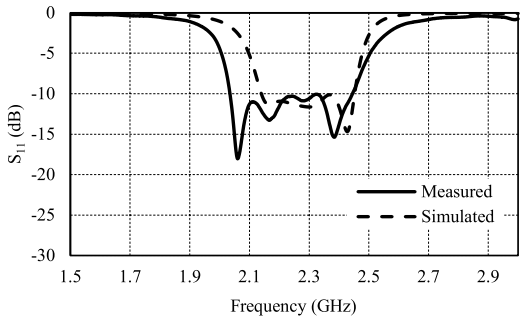

Figure 14.
Comparison of measured and simulated S_{11} performance.

bandwidth was 411, 2034–2445 MHz. The measured reflection coefficient of the antenna is compared with the simulated one in Figure 14, which shows a good agreement between the simulated and measured results. The measured impedance bandwidth is 100 MHz wider than the simulated one. It appears that the fabricated antenna became lossy due to the use of double-sided tape to attach several antenna layers to each other, which contributed to larger measured impedance bandwidth.

CONCLUSION

Compact CP antennas for CubeSats with wide AR bandwidth and beamwidth are critical for effective communication and science data download. A singly fed planar microstrip antenna is also desired for small satellite applications. This article presents stacked ring–patch antennas with negative and hybrid perturbations with wide angular beamwidths and AR bandwidths. These features are important for ground station access with increased coverage. These antennas can be used with NASA's NEN and DSN for high-speed data download in the *S*-band.

ACKNOWLEDGMENTS

This work was partially supported by the National Science Foundation under Award AGS 1936537.

REFERENCES

[1] S. Gao *et al.*, "Antennas for modern small satellites," *IEEE Antennas Propag. Mag.*, vol. 51, no. 4, pp. 40–56, Aug. 2009.

[2] Deep Space Network, 101 70-m Subnet Telecommunications Interfaces, Jet Propulsion Lab., California Inst. Technol., Pasadena, CA, USA, DSN No. 810-005, 101, Rev. E, Sep. 18, 2013.

[3] *Near Earth Network (NEN) User's Guide, 453-NENUG, Revision 4, Near Earth Network (NEN) Project, Code 453*, Goddard Space Flight Center, Greenbelt, MD, USA, Mar. 2019.

[4] S. Gao, Q. Luo, and F. Zhu, *Circularly Polarized Antennas*, 1st ed. New York, NY, USA: Wiley, 2014.

[5] H. M. Chen, Y. K. Wang, Y. F. Lin, C. Y. Lin, and S. C. Pin, "Microstrip-fed circularly polarized square-ring patch antenna for GPS applications," *IEEE Trans. Antennas Propag.*, vol. 57, no. 4, pp. 1264–1267, Apr. 2009.

[6] S. I. Latif and L. Shafai, "Circular polarization from dual-layer square-ring microstrip antennas," *IET Microw. Antennas Propag.*, vol. 6, no. 1, pp. 1–9, 2012.

[7] J. R. James, P. S. Hall, and C. Wood, *Microstrip Antenna Theory and Design*. London, U.K.: Peter Peregrinus,, 1981.

[8] I. J. Bahl and P. Bhartia, *Microstrip Antennas*, New York, NY, USA: Artech House, 1980.

[9] Z. Liu, L. Zhu, and X. Zhang, "A low-profile and high-gain CP patch antenna with improved AR bandwidth via perturbed ring resonator," *IEEE Antennas Wireless Propag. Lett.*, vol. 18, no. 2, pp. 397–401, Feb. 2019, doi: 10.1109/LAWP.2019.2892097.

[10] L. Sun, "A novel method of broadening bandwidth for compact single-fed circularly polarized microstrip antenna," in *Proc. IEEE Int. Conf. Microw. Millimeter Wave Technol.*, 2016, pp. 623–625, doi: 10.1109/ICMMT.2016.7762388.